Pure & Appl. Chem., Vol. 62, No. 9, pp. 1681–1688, 1990.
Printed in Great Britain.
© 1990 IUPAC

Deposition of amorphous silicon alloys

Jérôme PERRIN
Laboratoire de Physique des Interfaces et des Couches Minces
UPR A 0258 du C.N.R.S., Ecole Polytechnique, F-91128 - PALAISEAU Cedex, FRANCE

Abstract: Hydrogenated amorphous silicon alloys of carbon and germanium can be deposited by glow-discharge decomposition of gaseous hydrides or fluorides. Non-plasma methods such as photochemical vapour deposition are also used and offer guidelines for understanding and improving the standard glow-discharge method. These amorphous alloys usually have poorer structural and electronic properties than pure hydrogenated amorphous silicon but significant improvements can be obtained by different approaches such as hydrogen dilution of the gases, use of fluorides, selection of discharge conditions yielding predominantly XH_3 (X=Si,Ge,C) radicals, or moderate energy ion bombardment. The correlations between the film stoichiometry, microstructure and opto-electronic properties and the plasma gas-phase physico-chemistry and surface reaction kinetics are emphasized.

INTRODUCTION

With the development of technological applications of hydrogenated amorphous silicon (a-Si:H) semiconducting thin films in photovoltaic devices, it has been quickly recognized that large improvements in solar cell efficiencies are obtained by combining silicon-based alloys having larger or lower optical band-gaps than pure a-Si:H (1.7-1.75eV). Large band-gap materials are desirable as a front window in p-i-n junctions in order to prevent absorption of ultraviolet photons of the solar spectrum in the field-free p-layer. On the other hand, low band-gap materials are devoted to the absorption of red and near infrared photons either in single junction cells with graded band-gap intrinsic layer, or more likely in multilayer cells consisting of two or three stacked p-i-n junctions.

However, this improvement in terms of optical absorption should not be accompanied by a deterioration of electronic and hole transport properties which would ruin the carrier collection efficiency. Actually, it is rather easy to obtain large band-gaps in the silicon-carbon (a-Si:C:H) or silicon-nitrogen (a-Si:N:H) alloy systems, and low band-gaps in the silicon-germanium (a-Si:Ge:H) or silicon-tin (a-Si:Sn:H) systems, but the retention of the good electronic properties of a-Si:H appears more difficult. In this respect, a-Si:C:H is a better candidate than a-Si:N:H for large band-gap materials, and up to now, a-Si:Ge:H (F) alloys have acceptable electronic properties only down an optical gap of about 1.4 eV, whereas a-Si:Sn:H films are still improper for technological applications. As a matter of fact, it has been generally noticed that poorer electronic properties are associated with structural and microstructural defects. By microstructure we mean such aspects as columnar morphology, heterostructure (islands and tissue), voids (density deficiency) at a typical scale of 10nm. Structure and microstructure also involve hydrogen bonding type (SiH versus SiH_2 groups), hydrogen bonding strength (weakly or tightly bonded hydrogen), and hydrogen distribution (clustered or dispersed).

Here we present various methods used to synthetize group IV element silicon-based alloys, namely a-Si:C:H and a-Si:Ge:H(F). Microstructural and optoelectronic material properties are correlated to deposition conditions and plasma parameters. Then we try to interpret these correlations by investigating the plasma gas phase physico-chemistry, primarily in the case of rf-glow-discharge decomposition of molecular hydrides. Finally we analyze surface reaction mechanisms during film growth and outline the key factors leading to optimal material properties.

PREPARATION CONDITIONS

Diode glow-discharge PECVD

a-Si:C:H alloys are usually prepared by PECVD from mixtures of SiH_4 and CH_4 or other hydrocarbons such as C_2H_6, C_2H_4, C_2H_2 (ref. 1-6), in self-sustained diode dc or rf-glow discharges. Other compound gases have been used such as methylsilane $SiH_3\,CH_3$ (ref. 2) and even silylmethanes $CH_{3-n}(SiH_3)_n$ (ref. 7). In the case of a-Si:Ge:H alloys the usual gas mixture is SiH_4 and GeH_4 (ref. 8). a-Si:Sn:H films have also been obtained by glow discharge decomposition of SiH_4-$SnCl_4$ or $Sn(CH_3)_4$ gas mixtures (ref. 9). In any case, the substrate temperature is usually kept at 200-250°C and the deposition rate is of the order of 1Å/sec. Nevertheless, the simple plasma decomposition of hydrides often leads to a poor quality material as compared to pure a-Si:H.

Radical selection

A first answer to this problem has been to select the long-lived and less reactive radicals from the plasma, presumably SiH_3, CH_3, and GeH_3, in order to favour surface diffusion during film growth. For this purpose, the triode rf discharge concept has been proposed (ref. 10-12) where the plasma is confined by a grid electrode and the distance between the substrate electrode and the plasma source can be varied. The material quality is indeed improved, but the cost is a reduction of the deposition rate (typically 0.3Å/sec) as the grid-substrate distance increases. A similar improvement of material quality is obtained by using mercury sensitized photochemical vapour deposition as a selective source of XH_3 (X=Si,Ge) radicals (ref. 13-15). We also consider that the so-called "catalytic CVD" (ref. 16) belongs to the same category of techniques based on radical selection. In the latter case, the hydride molecule is decomposed at low pressure by heterogeneous pyrolysis on a high temperature filament and the reemitted radicals (presumably H + XH_3) diffuse and react on a substrate at T_s=200-250°C.

H_2 dilution and HRCVD

Owing to the limitations of the radical selection approach, the concept of H_2 dilution has been introduced (ref. 2,19) as a way to counteract H exodiffusion from the growing film surface and maintain the H-coverage of the surface for a better diffusion of XH_3 radicals. The material properties were indeed improved, especially for a-Si:Ge:H. Moreover, the H_2 dilution approach works very well in the conventional diode geometry. Nevertheless the deposition rate remains quite low as in the radical selection approach. However, This can be overcome by producing H radicals from a microwave source and feeding them in the conventional glow-discharge. This is the basis of the so-called hydrogen-radical-assisted-CVD (HRCVD) (ref. 20)

Fluorides

In spite of the relative success of the H_2 dilution approach, the use of fluorinated gases has been worked out by several groups (ref. 20-23). a-Si:C:H(F) was deposited from SiF_4 and C_2F_6 in H_2 (ref. 20), whereas a-Si:Ge:H(F) was obtained from SiH_4-GeF_4 or SiF_4- GeF_4-H_2 mixtures (ref. 20-23). In any case, hydrogen radicals still play a key role in the growth of a-Si alloys and the HRCVD technique has been combined with fluorides (ref. 20,21). Up to now the use of fluorides yield better a-Si:Ge alloys for optoelectronic applications than the simple H_2-dilution method.

Ion bombardment

Instead of the above-described "soft" chemical approaches, a completely different method for optimizing film growth conditions is the use of ion bombardment. It is now well established that the effect of ion bombarment depends on the range of kinetic energy, and that moderate energy ions (typically ≤50eV) drastically improve film growth conditions when the ratio of the ion flux (ϕ_+) to the total deposited atom flux (ϕ_0) is large enough ($\phi_+/\phi_0 \geq 10\%$). Such conditions are usually achieved in low pressure (10^{-3}- 10^{-2} Torr) plasmas. Indeed a clear demonstration of the beneficial effect of ion bombardment on the growth of a-Si:H has been given by using a magnetically confined multipole dc-discharges in pure SiH_4 between 0.5 and 4 mTorr (ref. 24). This was also verified in the case of a-Si:Ge:H deposited in a microwave (2.45 GHz) excited plasma of SiH_4-GeH_4 diluted in H_2 or in a rare gas at typically 1 mTorr (ref. 25). Large deposition rates up to 13 Å/sec have been achieved while keeping excellent optoelectronic properties of the material. More recently we have also analyzed the effect of ion bombardment on a-SiGe:H in a rf discharge of undiluted SiH_4-GeH_4 at 25mTorr by using a triode configuration with the substrate electrode placed 5mm behind the grid electrode and dc biased in order to vary the ion flux and energy without modification of the rf-discharge equilibrium (ref. 26). The value of ϕ_+/ϕ_0 was 20%.

MATERIAL PROPERTIES

Stoichiometry

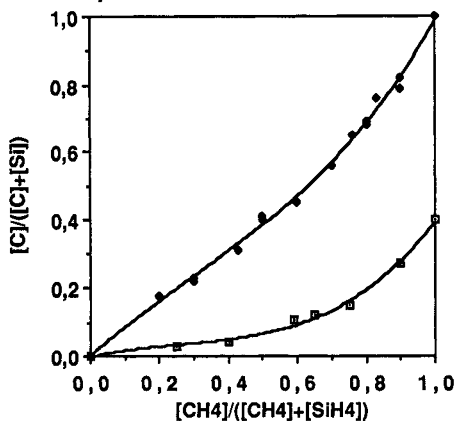

Fig. 1. Carbon incorporation in the film as a function of gas phase composition in a high power (♦) and a low power (▫) rf discharges (from ref. 6)

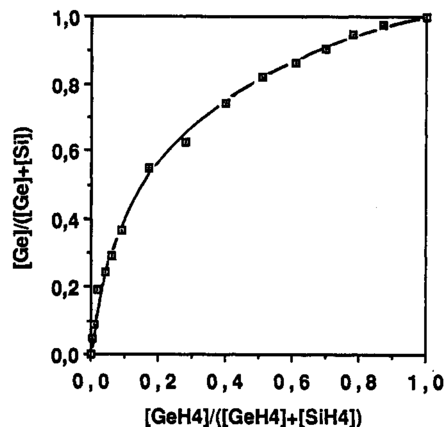

Fig. 2. Germanium incorporation in the film as a function of gas phase composition

The determination of absolute C or Ge content C_X=[X]/([X]+[Si]) in a film is not a trivial problem as shown in ref. 6 where C_C measured by various techniques (Rutherford backscattering, Auger electron and X-ray photoelectron spectroscopies, microprobe analysis, and direct chemical analysis) are compared. The direct chemical analysis was preferred and the variation of C_C as a function of the gas composition $R_g(CH_4)=[CH_4]/([CH_4]+[SiH_4])$ is shown in Fig. 1 for two rf-powers and a deposition temperature T_s=250°C. In the high power condition C_C increases almost linearly with R_g whereas in the low power condition C_C cannot exceed 40%. A striking result is that the deposition rate remains fairly insensitive to the partial and total silane pressure up to $R_g(CH_4) \approx 0.85$ where it vanishes.

The variation of C_{Ge}=[Ge]/([Ge]+[Si]) as a function of $R_g(GeH_4)$ is shown in Fig. 2 for films deposited at T_s=250°C at low discharge power. As opposed to the case of carbon, the Ge incorporation probability is here much larger than that of Si. Moreover the overall deposition rate tends to increase as a function of R_g. As expected, when increasing the discharge power, the preferential incorporation of Ge is reduced. An interesting feature in the case of a-Si:Ge:H(F) deposited from SiF_4-GeF_4-H_2 is that GeF_4 is much more easily dissociated than SiF_4 and H_2 so that a gas phase ratio $[GeF_4]/([SiF_4]+[GeF_4]) \approx 2\%$ yields $C_{Ge} \approx 0.50$

The C or Ge incorporation also depends on T_s. As shown in Fig. 3, the carbon incorporation probability decreases drastically from T_s=100°C to 200°C, whereas the opposite trend is observed for Ge.

Hydrogen incorporation and microstructure

The hydrogen incorporation in the film can be determined by nuclear reaction (^{11}B or ^{15}N), elastic recoil detection analysis (ERDA), IR absorbance, thermal evolution or direct chemical analysis. The H atomic content C_H=[H]/([X]+[Si]) increases as a function of carbon concentration in a-Si:C:H (refs. 2,3,5,6) reaching 80% for carbon rich films deposited at T_s =250°C. Fig. 4 shows that for Si rich films an empirical relationship holds $dC_H/dC_C \approx 3$, which suggests that C is incorporated mainly as CH_3 groups. Due to this specific preferential attachment of H on carbon the material deposited at low power should be labeled as "methylated amorphous silicon" (ref. 6). Solomon et al. (ref. 6) have shown that the low-power deposited "methylated amorphous silicon" is quite compact and stable. The presence of CH_2, CH_3 and $SiCH_3$ on IR absorbance spectra has been reported (refs.1,2). However, according to Matsuda et al. (ref. 2) such bonding configurations are associated to a low-density network and a high degree of disorder in the film, and correspond to the low temperature peak in hydrogen thermal evolution (ref. 3). They can be reduced when the films are deposited from H_2-diluted CH_4-SiH_4. The specificity of the "methylated amorphous silicon" probably comes from the fact that CH_3 groups are dispersed, avoiding microvoids and clustered polyhydride phase as in conventional a-Si:C:H.

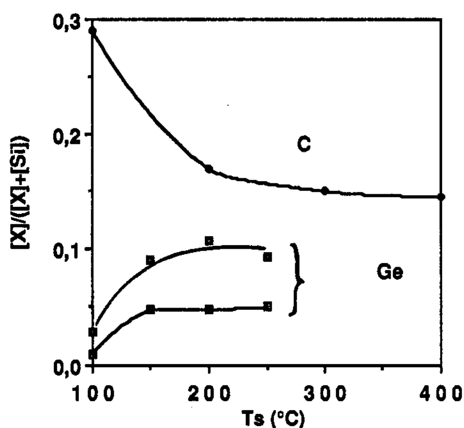

Fig. 3. Variation of [C]/[Si] and [Ge]/[Si] as a function of substrate temperature when keeping the same gas composition. Results for [C]/[Si] are from A. Matsuda (unpublished)

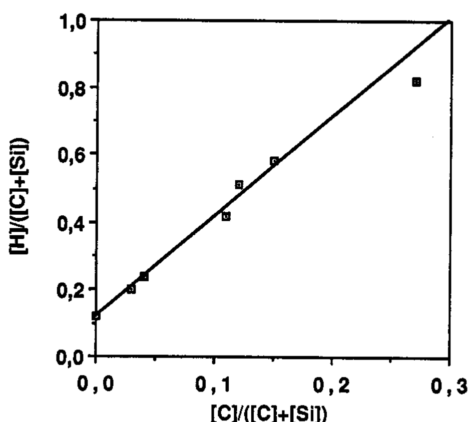

Fig. 4. H incorporation as a function of carbon concentration for films deposited at low-power (from ref. 6)

In a-SiGe:H films, the variation of the total H content as a function of C_{Ge} depends on the deposition temperature (ref. 27). For T_s<200°C, C_H increases with C_{Ge}, whereas C_H is constant or decreases for T_s> 200°C. Moreover the value of C_H also depends on other deposition parameters such as rf-power. In fact it has been shown that H is preferentially attached to Si (ref. 8), but the H bonding mode to Si is altered by the incorporation of Ge. This is illustrated in Fig. 5 showing the variation of H fractions bonded as SiH, SiH_2, GeH and GeH_2 groups. The transition from dominant SiH to dominant SiH_2 bonding modes is associated with a deterioration of the film microstructure as also revealed by the increase of the low temperature peak in hydrogen evolution spectra (ref. 3,27), the presence of microvoids and the larger volume fraction of low-density tissue relative to denser islands (ref. 28). However, when depositing the film with radical separation (ref. 10-12), H_2 dilution (ref. 17,19), fluorides (ref. 21,23) or ion bombardment (ref. 25,26), the transition from high density to low density microstructure is shifted to higher Ge content. The columnar microstructure disappears as shown by TEM (ref.12). Moreover the preferential attachment of H to Si is relaxed in favour of Ge. Indeed, on the IR absorbance spectra shown in Fig. 6 for films deposited with increasing ion bombardment energies, one can notice both the disappearance of components associated to SiH_2 groups and the relative enhancement of GeH components, although C_{Ge} remains constant

(ref. 26). Concerning a-Si:Ge:H(F) films deposited from fluorides, there has been a controversy as to whether F plays a beneficial role either in the deposition process or as a chemical constituent of the film. In fact the second hypothesis cannot hold since the F content is typically less than 1% (ref. 23).

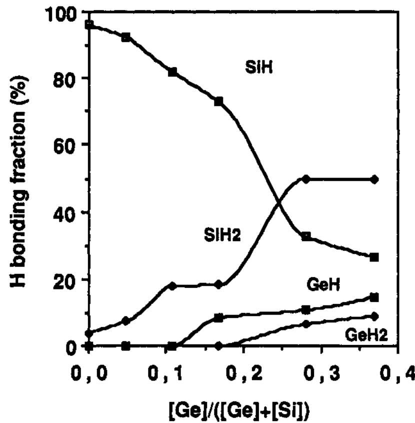

Fig. 5. Fractions of H in different bonding modes as a function of Ge content in the film for T_s=200°C

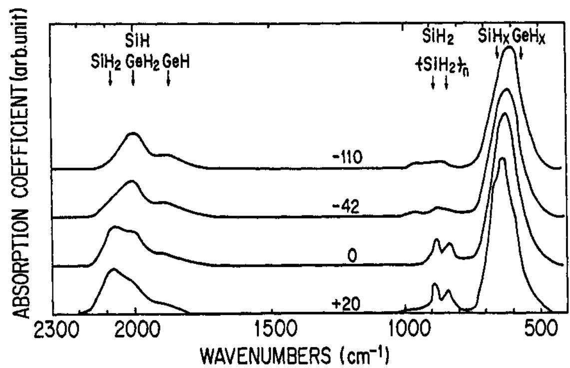

Fig. 6. IR absorbance spectra of a-Si:Ge:H films deposited at T_s=135°C for different substrate bias (from ref. 25)

Opto-electronic properties

The optical gap can be defined by the Tauc extrapolation method (E_{0T}) or by the photon energy at which the absorption coefficient $\alpha = 10^4$ cm^{-1} (E_{04}). For a-Si:H deposited at T_s=200-250°C, $E_{0T}\approx$1.70-1.75eV and $E_{04}\approx$1.9-1.95eV (typically $E_{04}\approx E_{0T}$+0.2eV). To a first approximation the refractive index and the optical gap are functions of the Si-C or Si-Ge stoichiometry. However the variations of H incorporation and film microstructure due to changes in T_s or plasma deposition conditions have a strong influence on the optical properties. For a film composition a-$Si_xGe_yH_z$ (x+y+z=1), a "universal" empirical relation has been found (ref. 19): E_{04}=1.795-0.75y+0.98z. However, in the case of films deposited at T_s=135°C under variable energy ion bombardment (ref. 26), both E_{0T} and E_{04} were found to decrease by almost 0.2 eV although the Ge content remained constant ($C_{Ge}\approx$0.37) and the H content decreased slightly. In the case of a-Si:C:H films, E_{04} can be increased up to 2.8 eV for the low power "methylated a-Si" containing a maximum carbon content C_C=0.4 (ref. 6).

Fig. 7 shows the relation between the dark conductivity σ_d and photoconductivity σ_{ph} under standard AM1 illumination versus the Tauc optical gap E_{0T} for a-Si:Ge:H(F) films deposited by various techniques. Although the decrease of σ_{ph} is very rapid for films deposited by the standard diode glow-discharge of SiH_4-GeH_4, both σ_{ph} and σ_{ph}/σ_d are significantly improved by using the triode radical separation technique. Further improvement is obtained by H_2 dilution. Finally the use of fluorides or the ion bombardment seem to provide the best photosensitive low-band gap material. In the case of a-Si:C:H films one can also observe a decrease of σ_{ph} as a function of C incorporation (ref. 2,3,28) and an improvement by using radical separation or H_2-dilution (ref. 2).

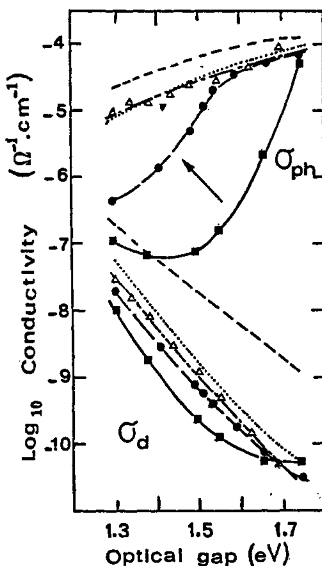

Fig.7. Dark conductivity σ_d and photoconductivity σ_{ph} as a function of Tauc optical gap E_{0T} for a-Si:Ge:H(F) films deposited by various techniques: diode glow discharge of SiH_4- GeH_4 (■), triode (●) and H_2-dilution (Δ) (from ref. 17), SiF_4-GeF_4-H_2 (--) (from ref. 23), and ion bombarment in low pressure microwave discharge (··) (from ref. 25). The arrow indicates the evolution of optoelectronic properties obtained by increasing the ion bombardment energy on a film deposited in a SiH_4- GeH_4 rf-discharge at T_s=135°C (ref. 26)

The origin of the degradation of optoelectronic properties in a-Si alloys lies in the microstructural film properties (see above), in the disorder created by alloying and in the presence of dangling bonds due preferential attachment of H. As a consequence, the density and distribution of localized electronic sates in the band gap, as measured by photothermal deflection spectroscopy (ref. 23,28,29) electron spin resonance (ref. 3,29), or space charge limited current (ref. 5) increases as a function of C (ref. 3,5,28) or Ge content (3,28,29) and is always larger than in pure a-Si:H in spite of the various improvement in the deposition techniques.

PLASMA GAS PHASE PHYSICO-CHEMISTRY

An excellent review of recent developments in the diagnostics and modelling of low pressure plasmas for the CVD of a-Si:H films was given by K. Tachibana at the previous ISPC-8 (ref. 30). Here we only compare some aspects of SiH_4, CH_4 and GeH_4 plasma decomposition relevant to a better understanding of the a-Si alloy film growth kinetics.

Excitation, dissociation and ionization of molecular hydrides by electron collisions

The variations of film growth rate and stoichiometry as a function of gas composition (see Fig. 1 and 2) are related first to electron-molecule inelastic collisions which govern the discharge equilibrium. We have measured the dissociation, ionization and emission cross-sections for 0-100eV electron impact on SiH_4 and GeH_4 and compared them to those for CH_4 (ref. 31-33). Emission cross-sections have been remeasured by another group (ref. 34). The more significant results are: i) the increase of the total inelastic cross-section at 100eV (dissociation into neutral + ionization) from CH_4 ($5.9\times10^{-16}cm^2$) to SiH_4 ($9.8\times10^{-16}cm^2$) and to GeH_4 ($19\times10^{-16}cm^2$); ii) the decrease of the ratio of the total ionization to the total dissociation cross section at 100 eV from nearly 1 for CH_4, to 0.5 for SiH_4, down to 0.3 for GeH_4; iii) the decrease of the ionization and dissociation potential and of the X-H bond energy and the evolution towards more fragmented products both in the ionization mass spectra and in the emission spectra where the relative contribution of molecular excited fragments (XH_2, XH and XH^+) to the UV-visible photon yield decreases to the benefit of excited X or X^+ atoms as shown in Fig. 8.

There have been some experimental and modelling studies of the respective dissociation degrees of each gas by using various diagnostics: mass spectrometry (ref. 1,36), IR laser absorption (ref. 4), CARS (ref. 35,37) and optical emission spectroscopy (ref. 35,36). The dissociation degree of CH_4 was found ≈10 times smaller than that of SiH_4 for $R_g(CH_4)=0.5$ at low power but decreases as the rf power increases, or as R_g decreases, or as the gas is more and more diluted in Ar (ref. 4). This is consistent with the dependence of the carbon incorporation in the film on R_g shown in Fig. 1 for low and high power. For GeH_4-SiH_4 mixtures, two studies (ref. 36,37) found that the dissociation rate of GeH_4 is 2.2 to 3 times larger than that of SiH_4 i.e slightly larger than the ratio of the total dissociation cross-sections ≈2 (ref. 32).

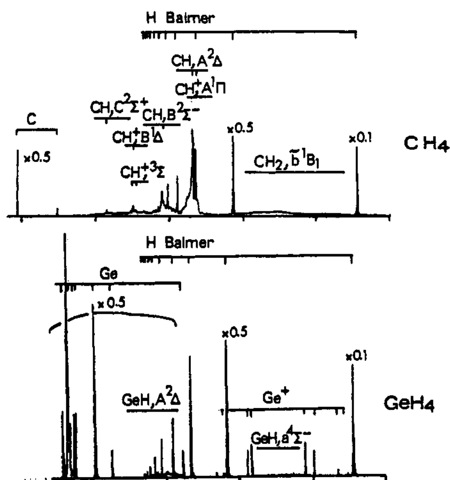

Fig.8. Emission spectra resulting from dissociative excitation of CH_4 and GeH_4 by 100 eV impact

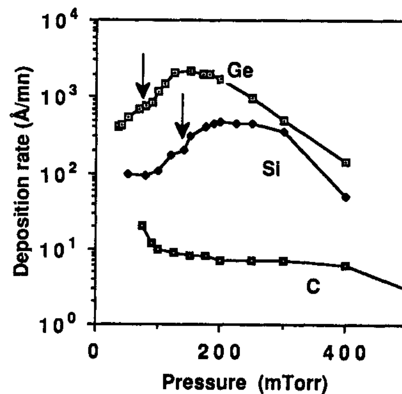

Fig. 9. deposition rate as a function of pressure for constant power (10 Watts) rf-discharges in CH_4, SiH_4, and GeH_4. The arrows indicate the α-γ transitions.

The α-γ transition in rf discharges

We have recently analyzed the transition between two rf-discharge regimes in SiH_4 and Si_2H_6 (ref. 38). In the low-pressure, low-power α-regime the power is dissipated by electrons gaining their energy by wave-riding at the oscillating sheath edges, whereas in the γ-regime, the acceleration of secondary electrons emitted at the electrodes takes over. The transition from the α to the γ-regime occurs by an electron avalanche in the sheath either by increasing the rf-voltage at a given pressure or by increasing the pressure at a given power and is characterized by a drastic increase of the deposition rate . We have shown that the pressure at which the α-γ transition occurs - provided the rf-power is large enough- can be predicted by the following expression:

$$P^*_{\alpha\gamma} = \left(\frac{243}{500}\right)^{1/4} \left\{\frac{\ln[(1+\gamma)/\gamma]}{2A}\right\}^{5/4} \left(\frac{1}{k_+\varepsilon_0}\right)^{1/2} \left(\frac{J_{0+}}{V_{sc}^{3/2}}\right)^{1/2}$$

where A is the preexponential factor in the Townsend semi-empirical expression for the ionization coefficient α, γ is the secondary electron emission coefficient, k_+ a constant in the expression of the high field ion mobility, J_{0+} the ion current density at the sheath edge and V_{sc} the sheath potential drop. The value of $P^*_{\alpha\gamma}$ for SiH_4 calculated from recent measurements of α (ref. 39) was found at 0.17 Torr in good agreement with the experimental results. This study is extended to the case of GeH_4 and CH_4 rf-discharges and we show in Fig. 9 the variation of deposition rate as a function of gas pressure for each gas at 10 Watts rf-power (≈0.1 $W.cm^{-2}$ on the electrode). It appears that the α-γ transition occurs at a lower pressure for GeH_4 than for SiH_4 whereas the transition is not apparent for CH_4 at this power. To a first approximation this can be attributed to the increase of both A and γ from CH_4 to SiH_4 and GeH_4 and to a decrease of the ratio $(J_{0+}/V_{sc}^{3/2})$. Further studies are necessary to elucidate these points. Nevertheless it is obvious that when varying the gas composition the critical pressure and power for the α-γ transition are shifted. In order to make relevant comparisons between discharges of different gas compositions it is important to know whether they are in the same regime. Indeed, when comparing SiH_4 and GeH_4 discharges both in the α-regime, the ratio of a-Ge:H to a-Si:H deposition rate is about 4 which is consistent within a factor of 2 with the total dissociation cross-section ratio, but this ratio becomes 20 when comparing at the same pressure (≈0.12 Torr) a GeH_4 discharge already in the γ-regime with a SiH_4 discharge still in the α-regime. One can also predict a shift to higher pressure of the α-γ transition upon dilution in H_2 or in a rare gas.

Ion and radical chemistry

There is little direct information on the ion and radical flux composition in gas-mixture discharges by in situ diagnostics (see e.g. ref. 1 for SiH_4-CH_4 discharges) but the pure SiH_4 and pure CH_4 plasma chemistries are well documented and already subject to modelling (ref. 30). Moreover some rate constants for GeH_n radicals are known. The following conclusions can be drawn:

i) the dominant neutral (resp. ionic) fragments of XH_4 molecules by electron impact are H (resp. H^+) and XH_3 and XH_2 (resp. XH_3^+ and XH_2^+) although the fraction of $XH_{n\leq 2}$ increases from C to Ge.

ii) the relative concentration of XH_3 and XH_3^+ increases with the pressure due to fast secondary reactions such as

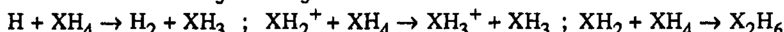

$$H + XH_4 \rightarrow H_2 + XH_3 \;;\; XH_2^+ + XH_4 \rightarrow XH_3^+ + XH_3 \;;\; XH_2 + XH_4 \rightarrow X_2H_6$$

The dominance of SiH_3 in moderate pressure SiH_4 discharges has been established recently by IR diode laser absorption (ref. 40). Relevant to this point is the interpretation of the deposition of "methylated a-Si" as due to the fact that there is no primary decomposition of CH_4 by electron impact in low power SiH_4-CH_4 discharges and that methyl radicals CH_3 or SiH_nCH_3 species are produced by secondary reactions of SiH_4 primary fragments (ref. 6),

iii) the relative XH_3 concentration is however limited in high power discharge by biradical recombination (ref.40)

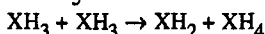

$$XH_3 + XH_3 \rightarrow XH_2 + XH_4$$

iv) the gas phase polymerization of positive and negative ions and radicals eventually lead to powder formation at high pressure

v) the ion to radical fraction, hence the ratio ϕ_+/ϕ_0, decreases as the pressure increases (ref. 38), which explains why ion bombardment is mostly effective in low pressure discharges

The effect of radical separation by using triode discharge has its origin in the difference of gas-phase reactivity between XH_3 and $XH_{n\leq 2}$ radicals. The ratio of XH_3 to $XH_{n\leq 2}$ fluxes is enhanced as the distance between the substrate and the grid increases (ref. 41). In the case of fluoride discharge it has been shown that the precursor for film growth are SiF_mH_n species produced by gas phase reactions between H and SiF_n radicals (ref. 20)

SURFACE PHENOMENA DURING FILM GROWTH

Film microstructure and surface reactivity of radicals

In situ and real-time studies of the growth process of a-Si:Ge:H films by ellipsometry (ref. 42) has revealed that the film microstructure (porosity and surface roughness) is related to the incomplete coalescence of nuclei at the early stages of deposition, and that the average surface roughness is larger for a-Ge:H than for a-Si:H. There is also a direct relation between surface roughness, columnar growth and polyhydride (XH_2 groups) incorporation, and the surface mobility and sticking probability of depositing species, as shown e.g. by phenomenological computer simulations (ref. 43).

The surface roughness is larger for films deposited in a multipole discharge at low pressure (<4mTorr), but with very low energy ions (<5eV) than for film deposited in rf-discharges in the α-regime (20-100mTorr). This shows that when ion bombardment is not involved the reactive species coming from a low pressure discharge -where the composition is primarily determined by electron impact fragmentation of XH_4 molecules and consist of significant fractions $XH_{n\leq 2}$ radicals and ions- have a much lower surface mobility and also a larger initial sticking probability than the XH_3 radicals which dominate at higher pressure due to gas-phase secondary reactions. Similarly, the disappearance of columnar morphology in a-Si:Ge:H films deposited in triode geometry is due to the enhancement of the XH_3 radicals relative contribution by radical separation (ref. 12, 41)

Sticking and recombination of XH_3 radicals

The origin of this difference in surface reactivity between XH_3 and $XH_{n\leq 2}$ has been ascribed to the fact that $XH_{n\leq 2}$ species can insert directly in the hydrogen covered surface of the growing film whereas XH_3 can only physisorb on surface X-H bonds. The rich H coverage of the surface has been demonstrated experimentally (ref. 44). We have proposed a surface reaction model for SiH_3 and GeH_3 on a-Si:H and a-Ge:H (ref. 14,15,45,46) in which

i) XH_3 is initially trapped in a physisorbed state on X-H bonds or reflected in the gas phase.
ii) Then the physisorbed XH_3 can diffuse on the surface by hopping on neighbouring X-H sites, or
iii) abstract an H atom and desorb as XH_4, thus creating a surface dangling bond X°.
iv) During diffusion two physisorbed XH_3 can recombine and desorb as X_2H_6.
v) Finally incorporation in the film occurs by chemisorption on a X° site.

According to this model we can define a surface loss probability β which involves a probability γ of recombination as XH_4 or X_2H_6 and s of sticking as illustrated in Fig. 10. β values lying typically between 0.1 and 0.3 for SiH_3 on a-Si:H and GeH_3 on a-Ge:H at low temperature have been determined (ref.14,15,45,46). The model also predicts that the ratio s/β should tends to 1 as the hydrogen coverage of the surface decreases. This has been verified by varying the H-coverage at a fixed temperature T_s using the catalytic effect of diborane (ref. 45). When increasing T_s both the H abstraction reaction and the surface hopping of XH_3 are activated, but the diffusion length becomes limited by the decrease of H coverage. The competition between H exodiffusion and surface mobility determines an optimum deposition temperature T_s and film microstructure for a given flux of reactive species. The variation of s/β as a function of T_s for SiH_3 is shown in Fig. 11. We also give the T_s dependence of $\beta(GeH_3)/\beta(SiH_3)$. The rapid increase of $\beta(GeH_3)$ above 150°C whereas $\beta(SiH_3)$ stays almost constant is due to the lower activation energy for H-abstraction from surface Ge-H bonds. This also explains why the [Ge]/[Si] ratio in a-Si:Ge:H films increases in the same T_s range (see Fig. 3) and why the film microstructure is poorer than for pure a-Si:H due to the reduction of both GeH_3 and SiH_3 surface mobility by Ge° dangling bonds. In the case of CH_3 versus SiH_3 surface kinetics we expect the opposite behaviour since the [C]/[Si] ratio decreases as a function of T_s (Fig. 3). However the fact that the film microstructure is also degraded by C incorporation suggest that the H-coverage is efficiently "scavenged" by CH_3 abstraction on Si-H sites and that the desorption of CH_4 is thermally activated (ref. 17). In this respect, the effect of H_2-dilution on the film growth both types of a-Si alloys can be understood not so much as a modification of gas phase chemistry in favour of XH_3 species than as a way to "fight" against the H-coverage deficiency by sending a high flux of H atoms on the growing surface (ref. 17).

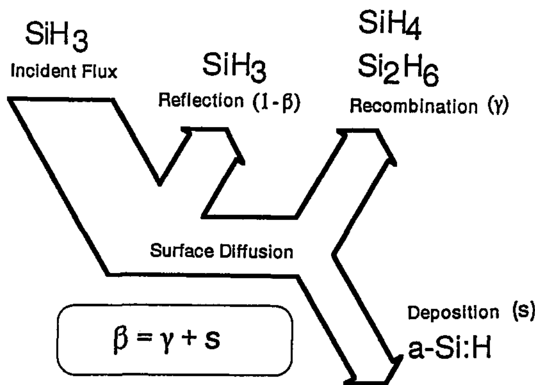

Fig. 10. Schematic concept of the surface reactions for SiH_3 radicals reaching the growing film H-covered surface

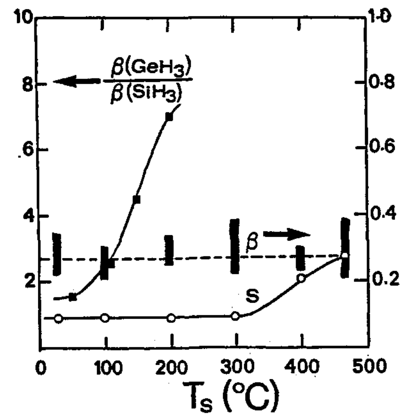

Fig. 11. Temperature dependence of β and s for SiH_3 (from ref. 46) and of the ratio $\beta(GeH_3)/\beta(SiH_3)$ (ref. 15)

The role of fluorine

Since F is only weakly incorporated in the film during deposition from fluorides diluted in H_2, the beneficial effect of F on the growth process has to be ascribed to surface reaction mechanisms. It has been suggested that SiF_mH_n gas-phase precursors (ref. 20) have a moderate sticking probability on the surface. Another hypothesis is that F acts as an etchant of the low-density polyhydride phase in the film microstructure, so that only the denser phase can grow. In any case F is finally eliminated from the surface as HF or SiF_mH_n stable species.

The effect of ion bombardment

When the reactive species incoming on to the surface are not selected according to their surface sticking probability and mobility, the only way to prevent the non mobile species to alter the film growth -as in low pressure discharge with no ion bombardment- is to give mobility to the adsorbed species by an external means such as photon irradiation or lateral momentum transfer by ion bombardment. The ion energy must remains low enough (typically ≤100eV) to avoid implantation and resputtering below the first few monolayers of the H-rich growth zone (ref. 44). Then, irrespective of the nature of incoming radicals, the growth of a dense network is favoured even at high deposition rate (ref.25). In addition ions can "scour" the weakest bonds of the polyhydride phase and erase the surface roughness as revealed by ellipsometry (ref. 42)

REFERENCES

[1] Y. Catherine and G. Turban, Thin Solid Films 60, 193-200 (1979); ibidem 76, 23-33 (1981).
[2] A. Matsuda, T. Yamaoka, S. Wolff, M. Koyama, Y. Imanishi, H. Kataoka, H. Matsuura, and K. Tanaka, J. Appl. Phys. 60, 4025-4027 (1986).
[3] W. Beyer, J. Non-Cryst. Solids 97&98, 1027-1034 (1987).
[4] K. Tachibana, H. Harima, and Y. Urano, ISPC-8, Tokyo, pp. 590-595 (1987).
[5] M.P. Schmidt, J. Bullot, M. Gauthier, P. Cordier, I. Solomon and H. Tran-Quoc, Phil. Mag. B 51, 581-589 (1985).
[6] I. Solomon, M.P. Schmidt, and H. Tran-Quoc, Phys. Rev. A 38, 9895-9901 (1988).
[7] H. Schmidbaur, R. Hager, J. Ebenhöch, and W. Beyer, Proc. of the Euroforum-New Energies Congress, Saarbrucken, pp. 124-126 (1988).
[8] W. Paul, D.K. Paul, B. Von Roedern, J. Blake, and S. Oguz, Phys. Rev. Lett. 46, 1016-1020 (1981).
[9] A.H. Mahan, D.L. Williamson, and A. Madan, Appl. Phys. Lett. 44, 220-222 (1984).
[10] A. Matsuda, K. Yagii, M. Koyama, Y. Imanishi, N. Ikuchi, and K. Tanaka, Appl. Phys. Lett. 47, 1061-1063 (1985).
[11] A. Matsuda, M. Koyama, N. Ikuchi, Y. Imanishi, and K. Tanaka, Jpn. J. Appl. Phys. 25, L54- (1986).
[12] T. Ichimura, T. Ihara, T. Hama, M. Oshawa, H. Sakai, and Y. Uchida, Jpn. J. Appl. Phys. 25, L276- (1986).
[13] M. Konagai, Mat. Res. Soc. Symp. Proc. 70, 257-268 (1986).
[14] J. Perrin, and T. Broekhuizen, Appl. Phys. Lett. 50, 433-436 (1987); Mat. Res. Soc. Symp. Proc. 75, 201-208 (1987).
[15] J. Perrin, and B. Allain, J. Non-Cryst. Solids 97&98, 261-264 (1987).
[16] H. Matsumura, Appl. Phys. Lett. 51, 804- (1987).
[17] A. Matsuda, and K. Tanaka, J. Non-Cryst. Solids 97&98, 1367-1374 (1987).
[18] L. Mariucci, F. Ferraza, D. Della Sala, M. Capizzi, and F. Evangelisti, J. Non-Cryst. Solids 97&98, 1075-1078 (1987).
[19] C. Godet, A. Lloret, and J.P. Stoquert, presented at the 9th E.C. Photovoltaic Solar Energy Conference, Freiburg, (1989).
[20] S. Oda, S. Ishihara, N. Shibata, H. Shirai, A. Miyauchi, K. Fukuda, A. Tanabe, H. Ohtoshi, J. Hanna, and I. Shimizu, Jpn. J. Appl. Phys. 25, L188-L190 (1986).
[21] S. Oda, S. Ishihara, N. Shibata, S. Takagi, H. Shirai, A. Miyauchi, and I. Shimizu, J. Non-Cryst. Solids 77&78, 877-880 (1985).
[22] K. Mackenzie, J. Hanna, J.R. Eggert, Y.M. Li, Z. Sun, and W. Paul, J. Non-Cryst. Solids 77&78, 1451-1460 (1985).
[23] D. Slobodin, S. Aljishi, Y. Okada, D.S. Shen, V. Chu, and S. Wagner, Mat. Res. Soc. Symp. Proc. 70, 275-281 (1986).
[24] B. Drévillon, J. Perrin, J.M. Siéfert, J. Huc, A. Lloret, G. de Rosny, and J.P.M. Schmitt, Appl. Phys. Lett. 42, 801-803 (1983).
[25] T. Watanabe, M. Tanaka, K. Azuma, M. Nakatani, T. Sonobe, and T. Shimada, Jpn. J. Appl. Phys. 26, L288-L290 (1987).
[26] J. Perrin, Y. Takeda, N. Hirano, H. Matsuura, and A. Matsuda, Jpn. J. Appl. Phys. 28, 5-11 (1989).
[27] G. Sardin, C. Roch, J. Andreu, J.L. Morenza, C. Godet, A. Lloret, and J.P. Stoquert, Proc. of the 8th E.C. Photovoltaic Solar Energy Conference, pp. 776-780, Kluwer Academic, Dordrecht (1988)
[28] H. Mahan, P. Raboisson, and R. Tsu, Appl. Phys. Lett. 50, 335-337 (1987).
[29] L. Chahed, M.L. Thèye, S. Basrour, J.C. Bruyère, C. Godet, and A. Lloret, Proc. of the 8th E.C. Photovoltaic Solar Energy Conference, pp. 846-850, Kluwer Academic, Dordrecht (1988)
[30] K. Tachibana, Pure & Appl. Chem. 60, 769-780 (1988).
[31] J. Perrin, J.P.M. Schmitt, G. de Rosny, B. Drévillon, J. Huc, and A. Lloret, Chem. Phys. 73, 383-394 (1982).
[32] J. Perrin, and J.F.M. Aarts, Chem. Phys. 80, 351-365 (1983).
[33] J. Perrin, and J.P.M. Schmitt, Chem. Phys. Lett. 112, 69-74 (1984).
[34] T. Sato, and T. Goto, Jpn. J. Appl. Phys. 25, 937-943 (1986); K. Tint, A. Kono, and T. Goto, ISPC-8, Tokyo, pp. 229-234 (1987).
[35] N. Hata, A. Matsuda, and K. Tanaka, J. Appl. Phys. 61, 3055-3060 (1987).
[36] H. Chatham, and P.K. Bhat, Proceedings of the MRS spring meeting, Reno 1988, to be published
[37] J.W. Perry, Y.H. Shing, and C.E. Allevato, Appl. Phys. Lett. 52, 2022-2024 (1988).
[38] J. Perrin, P. Roca i Cabarrocas, B. Allain, and J.M. Friedt, Jpn. J. Appl. Phys. 27, 2041-2052 (1988).
[39] M. Shimozuma, and H. Tagashira, J. Phys. D 19, L179-L182 (1986).
[40] N. Itabashi, K. Kato, T. Goto, C. Yamada, and E. Hirota, Jpn. J. Appl. Phys. 28, L325-L328 (1989).
[41] A. Matsuda, and K. Tanaka, J. Appl. Phys. 60, 2351-2356 (1986).
[42] A.M. Antoine, B. Drévillon, and P. Roca i Cabarrocas, J. Appl. Phys. 61, 2501-2508 (1987).
[43] M.J. McCaughey, and M.J. Kushner, J. Appl. Phys. 65, 186-195 (1989).
[44] G.H. Lin, J.R. Doyle, M. He, A. Gallagher, J. Appl. Phys. 64, 188-194 (1988).
[45] J. Perrin, Y. Takeda, N. Hirano, Y. Takeuchi, and A. Matsuda, Surf. Sci. 210, 114- 128 (1989).
[46] A. Matsuda, K. Nomoto, Y. Takeuchi, A. Suzuki, A. Yuuki, and J. Perrin, Surf. Sci. (to appear)